

# Joint Charging and Rate Allocation for Utility Maximization in Sustainable Sensor Networks

Zi Li, Yang Peng, Daji Qiao, and Wensheng Zhang  
 Iowa State University, Ames, IA 50011  
 Email: {zili, yangpeng, daji, wzhang}@iastate.edu

**Abstract**—A sensor network deployed for long-term monitoring shall sustain meanwhile provide as much useful sensory information (i.e., as high network utility) as possible. We propose a JCRA (Joint Charging and Rate Allocation) scheme to maximize the network utility while satisfying the network sustainability requirement. JCRA is designed based on the observation that the energy repository of a sensor node is co-affected by three factors: uncontrollable ambient energy harvesting, controllable wireless charging, and controllable sensory data generation. It jointly controls the charging, communication, and sensing activities while guaranteeing non-empty energy repositories at all sensor nodes. JCRA is a low-cost solution, as neighbor sensor nodes collaborate with each other to adjust their data generation rates in a distributed manner, based on the status of ambient energy supply and the wireless charging schedule planned by the base station. Extensive simulations have verified the effectiveness of JCRA in achieving the stated goals: JCRA can always guarantee network sustainability, while the achieved network utility is close to that by a centralized  $(1 - \epsilon)$  approximate solution to the same optimization problem, in most simulation settings.

## I. INTRODUCTION

For a sensor network deployed for long-term monitoring, it is critical that the network sustains meanwhile provides as much useful sensory information as possible. Due to limited energy supply at the deployment time, perpetual energy replenishment is needed. Harvesting ambient energy such as solar [1], wind [2], and vibration [3] has been a cost-free but uncontrollable approach for energy replenishment; the emerging wireless charging technology [4] has posed as a controllable approach [5], [6] but needs extra hardware support. As these approaches are complementary to each other, a natural idea is to integrate them together, and within the integration, the ambient energy source shall be fully exploited while the wireless charging source shall be utilized efficiently.

To measure how much useful information the network can provide, *network utility* has been introduced as a performance metric. To provide as much useful information (i.e., high network utility) as possible, the sensor nodes shall sense frequently and report the sensory data in a timely and lossless manner. This way, however, energy could be consumed rapidly, and the loss of energy may not be compensated soon enough to keep the network functional. Hence, the goals of network sustainability and maximization of network utility could conflict with each other and need to be considered together.

In this paper, we propose a distributed and practical scheme

called JCRA (Joint Charging and Rate Allocation) that jointly control the wireless energy charging activities and the sensory data generation at sensor nodes, so as to maximize the network utility while guaranteeing the network sustainability. Specifically, in JCRA, sensor nodes periodically report their status to the base station (BS). Based on the collected information, the BS schedules the charging activities of the mobile charger (MC) and disseminates the charging schedule to the network. At the meantime, based on the received charging schedule, each sensor node collaborates with its neighbors to adjust their data generation rates locally in the distributed manner, with the target of improving the total utility within the neighborhood. As such collaboration occurs in all neighborhoods, the overall utility of the network is improved gradually.

The results of extensive simulations have verified that JCRA can effectively achieve the dual goals of network sustainability and high network utility. Particularly, in most of the simulation settings, the performance of JCRA is close to that of a centralized  $(1 - \epsilon)$  approximate solution to the same optimization problem. The contributions of this work can be summarized as follows. First of all, different from existing works [4]–[16], JCRA is the first work that considers together the following three factors: uncontrollable ambient energy harvesting, controllable wireless charging, and controllable sensory data generation, to maximize network utility while sustaining the network. For detailed comparison between JCRA and existing works, please refer to Section VI. Secondly, we formulate the joint charging and rate allocation optimization problem and develop a centralized,  $(1 - \epsilon)$  approximate solution to the problem, which provides a theoretical foundation to the design and evaluation of the proposed JCRA scheme. Finally, JCRA has been thoroughly evaluated via ns-2 simulations. Results show that it approaches the network utility achieved by the centralized,  $(1 - \epsilon)$  approximate solution, under various network settings while satisfying the sustainability requirement.

In the following, Sections II and III present system models and analytical study. The JCRA design is elaborated in Section IV. Section V reports evaluation results. Section VI reviews related works and Section VII concludes the paper.

## II. SYSTEM MODELS

We consider a system (as illustrated by Figure 1) composed of a network of  $N$  sensor nodes each equipped with both wireless energy receiver and ambient energy harvesting devices, a base station (BS), and a mobile charger (MC).

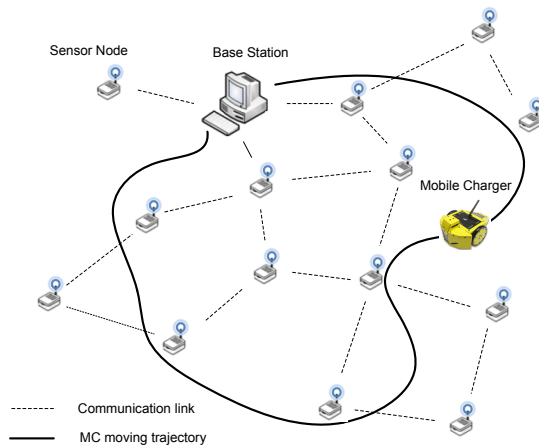


Fig. 1. System Overview.

The sensor nodes form a data collection tree rooted at the BS. Each node generates sensory data and forwards the data generated by itself and its descendants on the tree towards the BS. Besides harvesting ambient energy, each node can also receive energy wirelessly charged from the MC. The BS collects the status of each sensor node, computes a charging schedule for the MC, and commands the MC via a long range radio to execute the schedule. Based on the schedule, the MC travels along a predefined trajectory to charge sensor nodes. Charging activities are scheduled and executed round by round. In each round, the MC starts from the BS with a full energy battery, moves along the trajectory, stops at designated locations to charge sensor nodes, and returns to the BS to replace battery before its energy is depleted.

### A. Wireless Charging Model

We assume that the MC only conducts charging when it stops at certain points along the trajectory  $S$ . According to the experiments in [12], the efficiency for charging energy from the MC at point  $s$  to node  $i$  over a distance of  $d(i, s)$  is

$$\eta_i(s) = -0.0958 * d^2(i, s) - 0.0377d(i, s) + 1.0. \quad (1)$$

Therefore, the amount of power received by node  $i$  when the MC is at point  $s$  is

$$\Lambda_i(s) = \begin{cases} \eta_i(s)\Lambda_c & : d(i, s) \leq d_{\max}, \\ 0 & : \text{otherwise,} \end{cases} \quad (2)$$

where  $\Lambda_c$  is the charging power output at the MC and  $d_{\max}$  is a distance threshold, over which only a negligible amount of energy can be transferred. We also assume that wireless charging and communication do not interfere with each other.

### B. Network Utility Model

To quantify the usefulness of sensory data generated by each node  $i$  to an application, we assume the application provides a utility function  $U(r_i)$ , where  $r_i$  is the data packet generation rate at node  $i$ . In many sensor network applications [11], [17], [18], the utility function is expected to have a *diminishing return* property which means that the usefulness of sensory data generated by a node increases as the data

rate increases, but in a sub-linear fashion. For example, in an intruder detection application, once the sensory data generation rate has reached a certain threshold, the amount of new information that can be obtained through increasing the data rate further at a sensor node only increases sub-linearly. Hence, we assume  $U(\cdot)$  is a non-decreasing, concave function; that is,  $\forall \Delta > 0$ ,  $U(x + \Delta) - U(x) > U(y + \Delta) - U(y)$  if and only if  $x < y$ . The overall network utility is  $\sum_{i=1, \dots, N} U(r_i)$ .

### C. Problem Statement

In this study, we aim to maximize the network utility under the constraint that the sensor network sustains (i.e., each node has a non-empty nodal energy repository at any time). As illustrated in Figure 2, the energy repository of a node is co-affected by two energy producers (i.e., uncontrollable ambient energy source and controllable wireless charger) and one energy consumer (i.e., the node itself that conducts controllable local communication and sensing activities).

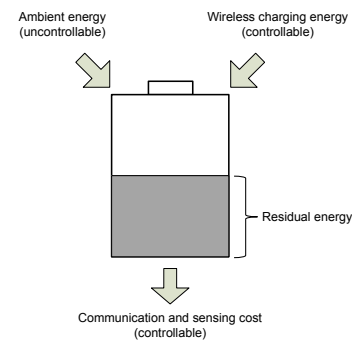


Fig. 2. The three actors co-affect the nodal energy repository.

Hence, the problem is, given the uncontrollable ambient energy supply, how to jointly control the charging, communication, and sensing activities to maximize the network utility meanwhile guarantee non-empty energy repositories at all nodes. More specifically, it can be stated as follows:

#### Objective:

- $\max \sum_{i=1, \dots, N} U(r_i)$ .

#### Inputs:

- Data collection tree:  $T$ ;
- Entire moving trajectory of the MC:  $S_{\text{full}}$ ;
- Length of a charging round:  $I_{\text{round}}$ ;
- Initial nodal energy:  $e_i(0)$  for each node  $i$  ( $i = 1, \dots, N$ );
- Ambient energy harvesting rate:  $\hat{H}_i$  for each node  $i$ ;
- Utility function:  $U(\cdot)$ .

#### Outputs:

- Charging schedule:  $a(s)$  for  $s \in S_{\text{full}}$ , where  $a(s)$  is the amount of time that the MC conducts charging at point  $s$  on  $S_{\text{full}}$ ;

- Nodal data generation rate:  $r_i(t)$  for each node  $i$ .

**Subject to:**

- Nodal residual energy  $e_i(t) > 0$  at any time  $t$ .

Here, we assume the moving speed of the MC (denoted as  $v_{MC}$ ) is constant. Hence, as the moving trajectory of the MC (i.e.,  $S_{\text{full}}$ ) is fixed, the time for the MC to travel the entire trajectory is fixed. We also assume the charging power output of the MC ( $\Lambda_c$ ) is constant. Therefore, the overall amount of energy available for the MC to charge to sensor nodes during a charging round is  $\left(I_{\text{round}} - \frac{|S_{\text{full}}|}{v_{MC}}\right) \Lambda_c$ .

### III. ANALYTICAL STUDY AND CENTRALIZED $(1 - \epsilon)$ APPROXIMATE SOLUTION

Directly solving the afore-stated problem is difficult because the moving trajectory is continuous and a prohibitively large space of feasible solutions need to be searched in order to find the optimal one. Hence, we construct an approximate solution in this section. Specifically, we first present a problem formulation in which the continuous moving trajectory is discretized into a finite sequence of segments and each segment is represented by a point. Based on this formulation, we then develop an approximate solution that provides a provable  $(1 - \epsilon)$  approximation ratio, where parameter  $\epsilon$  stands for an adjustable inaccuracy level.

#### A. A Discretized Problem Formulation

We have formulated a generic discretized problem for any moving trajectory of the MC, denoted as  $S$ , and any time duration of the MC movement, denoted as  $\omega$ .  $S$  is discretized into a set of  $K$  equal-length segments, and each segment is represented by its geometric central point. The problem can be formally described as follows:

**Objective:**  $\max \sum_i U \left( \frac{\sum_{k=1}^K g_i(s_k)}{\omega} \right)$ .

**Inputs:**  $T, S, \omega, \{e_i, \hat{H}_i | 1 \leq i \leq N\}, U(\cdot)$ , and  $K$ .

**Outputs:**  $\left\{ a(s_k), r_i(s_k) = \frac{g_i(s_k)}{\omega(s_k)} \mid 1 \leq k \leq K; 1 \leq i \leq N \right\}$ .

**Subject to:**

$$\sum_{k=1}^K \omega(s_k) \leq \omega, \quad (3)$$

$$\omega(s_k) = \frac{\ell(s_k)}{v_{MC}} + a(s_k), \quad (4)$$

$$c_i(s_k) = \sum_{\forall j \in D_i} (e_{tx} + e_{rx})g_j(s_k) + (e_{tx} + e_{sx})g_i(s_k), \quad (5)$$

$$e_i(s_{k+1}) \leq e_i(s_k) - c_i(k) + \hat{H}_i \omega(s_k) + a(s_k) \Lambda_i(s_k). \quad (6)$$

$$0 < e_i(s_k) \leq E_{\text{max}}, \quad (7)$$

$$a(s_k) \geq 0. \quad (8)$$

This is a generic formulation that works for any  $S$  and  $\omega$ . Comparing to the original problem, this formulation has a new input  $K$  which represents the number of segments that the continuous trajectory should be divided into. The outputs include the charging schedule and the nodal sensory data generation rates. Particularly, the charging schedule is represented as a set of  $a(s_k)$  for  $k = 1, \dots, K$ , where  $a(s_k)$  is the charging time spent by the MC at each segment  $s_k$ . The objective is to maximize the network utility during a time period of  $\omega$ , where  $g_i(s_k)$  is the number of data packets generated by node  $i$  when the MC is at segment  $s_k$ . As stated in Equation (3), the overall time spent by the MC at all segments, i.e.,  $\sum_{k=1}^K \omega(s_k)$ , shall be less than or equal to the time period of  $\omega$ .  $\omega(s_k)$  includes two parts: the  $\frac{\ell(s_k)}{v_{MC}}$  time spent by the MC to traverse segment  $s_k$  and the  $a(s_k)$  time spent by the MC to charge, where  $\ell(s_k)$  is the length of  $s_k$  and  $v_{MC}$  is the MC's moving speed. Equation (5) computes the amount of energy consumed by node  $i$  when the MC is within  $s_k$ . Here, the energy costs to transmit, receive, and generate a data packet are denoted as  $e_{tx}$ ,  $e_{rx}$ , and  $e_{sx}$ , respectively. In Inequality (6), the residual energy  $e_i(s_{k+1})$  of node  $i$  shall be no more than  $e_i(s_k)$  (the residual energy of node  $i$  when the MC enters  $s_k$ ), plus the amount of energy harvested and charged during the time period that MC is within  $s_k$ , and minus the amount of energy consumed by the node during the same period. Here,  $\hat{H}_i$  and  $\Lambda_i(s_k)$  are the average ambient energy harvesting rate and energy charging rate at node  $i$  when the MC stays at  $s_k$ , respectively. Equation (7) states that the residual energy of each node shall be larger than zero (i.e., the sustainability requirement) and less than the battery capacity. Equation (8) ensures that the charging time at each segment shall be larger than or equal to zero. Based on the facts that (i) all constraints in the formulation are linear, (ii) utility function  $U(\cdot)$  is a non-decreasing concave function, and (iii) sum of concave functions is also concave, the above formulation is a convex optimization problem. A solver such as [19] can be used to solve it.

#### B. An Approximate Algorithm

Following the strategy developed in [6], this section constructs an approximate algorithm to approach the original optimization problem stated in Section II. The approximation is based on the discretized problem formulated in Section III-A. The pseudo code of the algorithm is given in Algorithm 1. We will prove that, by plugging in  $S = S_{\text{full}}$  and  $\omega = I_{\text{round}}$  as part of the inputs, this algorithm provides a  $(1 - \epsilon)$  approximate solution to the original problem.

$K$  is a key parameter that affects how close the output of our algorithm is to the optimal solution to the original problem. In order to determine an appropriate  $K$  value that gives a  $(1 - \epsilon)$  approximation, the algorithm adopts the following iterative method: starting from  $K = 2$ , every iteration doubles  $K$ ; in each iteration, the lower and upper bounds of the solution to the discretized problem are computed, and the difference between the two bounds is calculated; the iterative process continues till the bound difference becomes smaller than  $\epsilon$ .

In the following, we first discuss how to compute the lower

**Algorithm 1** Centralized  $(1 - \epsilon)$  Approximate Solution**Inputs:**  $T, S, \omega, \{e_i, \hat{H}_i | 1 \leq i \leq N\}, U(\cdot)$ .**Outputs:**  $K, \{a(s_k), r_i(s_k) | 1 \leq k \leq K; 1 \leq i \leq N\}$ 

- 1:  $K \leftarrow 1$
- 2: **repeat**
- 3:    $K \leftarrow 2 \times K$
- 4:   Evenly divide  $S$  into  $K$  segments  $s_1, \dots, s_K$
- 5:   Solve the discretized problem (Section III-A) with inputs of  $T, S, \omega, \{e_i, \hat{H}_i | 1 \leq i \leq N\}, U(\cdot)$  and  $K$ , and  $\Lambda_i(s_k)$  replaced with  $\Lambda_i^l(s_k) = \min_{p \in s_k} \Lambda_i(p)$  in Equation (6) to output  $\{a^l(s_k), r_i^l(s_k) | 1 \leq k \leq K, 1 \leq i \leq N\}$
- 6:   The objective value associated with the solution is assigned to  $LB(K)$
- 7:   Solve the discretized problem (Section III-A) with inputs of  $T, S, \omega, \{e_i, \hat{H}_i | 1 \leq i \leq N\}, U(\cdot)$  and  $K$ , and  $\Lambda_i(s_k)$  replaced with  $\Lambda_i^u(s_k) = \max_{p \in s_k} \Lambda_i(p)$  in Equation (6) to output  $\{a^u(s_k), r_i^u(s_k) | 1 \leq k \leq K, 1 \leq i \leq N\}$
- 8:   The objective value associated with the solution is assigned to  $UB(K)$
- 9:   **until**  $\frac{LB(K)}{UB(K)} > 1 - \epsilon$
- 10: **return**  $K, \{a^l(s_k), r_i^l(s_k) | 1 \leq k \leq K, 1 \leq i \leq N\}$

and upper bounds and then explain how the algorithm achieves the desired  $(1 - \epsilon)$  approximation ratio. Considering any segment  $s_k$  and any node  $i$ , the energy charging rate of node  $i$  differs when the charger operates from different points on  $s_k$ . Given a  $K$  value, the lower bound of the solution to the discretized problem can be computed as the solution when  $\Lambda_i(s_k)$  for each node  $i$  is replaced with  $\Lambda_i^l(s_k) = \min_{p \in s_k} \Lambda_i(p)$  (i.e., the minimum charging rate at node  $i$  if the charger is allowed to operate from any point on  $s_k$ ) in Equation (6). Similarly, the upper bound can be computed as the solution when  $\Lambda_i(s_k)$  is replaced with  $\Lambda_i^u(s_k) = \max_{p \in s_k} \{\Lambda_i(p)\}$  in Equation (6). We denote the computed lower and upper bounds as  $LB(K)$  and  $UB(K)$ , respectively, in the algorithm.

Because the lower (upper) bound increases (decreases) as the algorithm iterates (which will be proved in Lemma 3.1 below), when the algorithm terminates, we have the following relation:

$$LB(K) \leq LB(\infty) = UB(\infty) \leq UB(K), \quad (9)$$

and

$$\frac{LB(K)}{UB(K)} > 1 - \epsilon. \quad (10)$$

On the other hand, we know that, as  $K$  approaches  $\infty$ , the solution to the discretized problem becomes the solution to the original continuous problem. This means that the output of our algorithm is a  $(1 - \epsilon)$  approximate solution to the original continuous problem.

*Lemma 3.1:* As  $K$  increases,  $LB(K)$  increases and  $UB(K)$  decreases.

*Proof:* (By construction). When  $K$  is increased to  $2K$ , each segment  $s_k$  for  $1 \leq k \leq K$  is split into two equal-length smaller segments  $s_k^1$  and  $s_k^2$ . For each node  $i$ , it holds that  $\Lambda_i^l(s_k) \leq \Lambda_i^l(s_k^1)$  and  $\Lambda_i^l(s_k) \leq \Lambda_i^l(s_k^2)$ . Hence,  $LB(K)$  which is the solution to the discretized problem with  $\Lambda_i(s_k) = \Lambda_i^l(s_k)$  in Equation (6) is no greater than  $L(2K)$  which is the solution

to the discretized problem with  $\Lambda_i(s_k^1) = \Lambda_i^l(s_k^1)$  and  $\Lambda_i(s_k^2) = \Lambda_i^l(s_k^2)$  in Equation (6), while other conditions are the same for these two versions of the problem. Hence, it is proved that  $LB(K) \leq LB(2K)$ , that is,  $LB(K)$  increases as  $K$  increases. Similarly, it can be proved that  $UB(K) \geq UB(2K)$ , that is,  $UB(K)$  decreases as  $K$  increases. ■

## IV. THE PROPOSED JCRA SCHEME

Although Algorithm 1 provides a nice solution to the problem with a provable  $(1 - \epsilon)$  approximation ratio, it is a centralized algorithm; thus, dissemination of the node-specific rate information requires a unicast from the BS to each sensor node in the network. This could incur a very high communication overhead as the network size increases, which limits its applicability in practice. In this section, we present JCRA (Joint Charging and Rate Allocation) – a distributed, localized, and low-cost solution, with which (i) the BS determines the charging schedule of the MC based on the status information reported by sensor nodes; while (ii) each sensor node collaborates with its neighbors to adjust their data generation rates locally in a distributed manner. Details of the base station and sensor node behaviors are elaborated next.

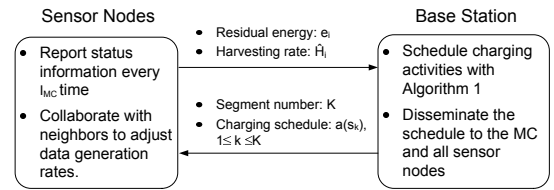


Fig. 3. Overview of the JCRA scheme.

## A. Base Station Behavior

As shown in Figure 3, every  $I_{MC}$  time, each sensor node  $i$  reports the following information to the BS: current residual energy  $e_i$  and estimated future ambient energy harvesting rate  $\hat{H}_i$ . Based on these information, the BS determines the charging schedule of the MC for the rest of the current charging round, by executing Algorithm 1 with the following as the inputs: (i) updated  $e_i$  and  $\hat{H}_i$  information for each sensor node  $i$ ; (ii)  $\omega$ : the remaining time of the current charging round; and (iii)  $S$ : the remaining trajectory to be traversed in the current charging round. As the output of the algorithm, the charging schedule of the MC includes: (i) an updated  $K$  value: the number of segments for the remaining trajectory; and (ii) updated  $a(s_k), 1 \leq k \leq K$ : the amount of charging time that the MC shall spend at each segment.

Next, the BS disseminates the newly-determined charging schedule to the MC and all sensor nodes in the network. The updated charging schedule will help sensor nodes adjust their data generation rates during the next  $I_{MC}$  interval; details will be discussed in the next section.

## B. Sensor Node Behavior

In JCRA, neighbor sensor nodes exchange lightweight control information between each other and adjust their data

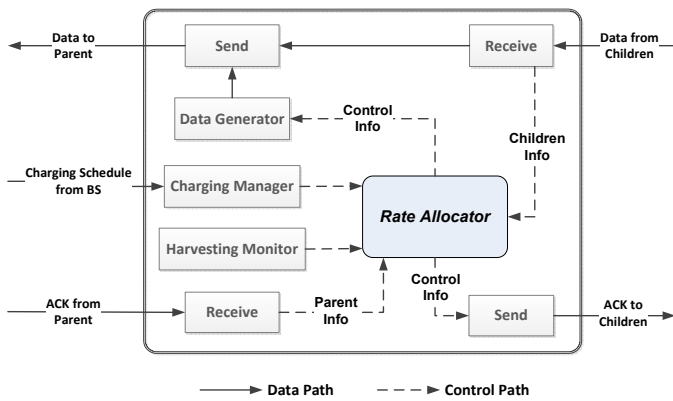


Fig. 4. Overview of the sensor node behavior in JCRA.

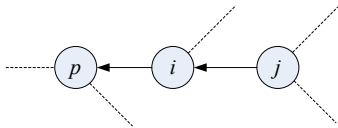


Fig. 5. Topology used to describe JCRA details.

generation rates together in a collaborative manner. As coordinations only take place locally between neighbors, the goal becomes to maximize the total utility within the neighborhood rather than the entire network. However, as such procedure occurs in all neighborhoods, the overall utility of the entire network can be improved gradually.

*1) Design Overview:* Figure 4 gives an overview of the sensor node behavior. To ease the presentation, we use the topology shown in Figure 5 as an example to explain the design details. In general, when node  $i$  receives a data packet from its child nodes or an ACK from its parent node, it extracts the following control information embedded in the packet and feeds them into the *Rate Allocator* module: (i) from each child node  $j$  of  $i$ :  $\hat{e}_j$  ( $j$ 's estimated residual energy at the end of the current charging round) and  $r_j$  ( $j$ 's current data generation rate); and (ii) From the parent node  $p$  of  $i$ : *rate adjustment token* – denoted by  $\Delta_{p,i}$ . Here, *rate adjustment token* is an important variable in the proposed JCRA scheme. Node  $p$  uses a rate adjustment token  $\Delta_{p,i}$  to notify node  $i$  whether it is able to handle additional traffic from the subtree rooted at node  $i$ .  $\Delta_{p,i}$  could have one of the following three values:  $+\delta$ ,  $-\delta$ , or 0, where  $\delta$  is a system parameter.  $\Delta_{p,i} = +\delta$  represents that node  $p$  can handle additional  $\delta$  amount of traffic from the subtree rooted at node  $i$  without violating the sustainability requirement, while  $\Delta_{p,i} = -\delta$  indicates that node  $p$  has been overloaded and the traffic from the subtree rooted at node  $i$  shall be reduced.  $\Delta_{p,i} = 0$  means node  $i$  and its decedents are allowed to adjust their data generation rates as long as the overall traffic rate from node  $i$  remains unchanged.

The *Harvesting Monitor* module is responsible for estimating the following values: (i)  $e_i$ : node  $i$ 's current residual energy; and (ii)  $\hat{H}_i$ : node  $i$ 's future ambient energy harvesting rate. Note that schemes like [20] may be employed to estimate  $\hat{H}_i$  based on historical energy harvesting profiles. In addition, when the *Charging Manager* module receives a new charging schedule from the BS, it updates the following information and

provides to the *Rate Allocator* module: (i)  $\omega$ : the remaining time of the current charging round; and (ii)  $\hat{A}_i$ : the amount of energy that node  $i$  can be charged in  $\omega$  time, which is calculated as

$$\hat{A}_i = \sum_{k=1}^K a(s_k) \Lambda_i(s_k), \quad (11)$$

where  $\Lambda_i(s_k)$  is the charging rate for node  $i$  when the MC operates at the central point of segment  $s_k$ . Formula to calculate  $\Lambda_i(s_k)$  is given in Equation (2).

With all the above information, the *Rate Allocator* module decides how node  $i$  shall adjust its data generation rate as well as the values of the rate adjustment tokens that node  $i$  shall pass to its child nodes, which are discussed next.

*2) Rate Adjustment Process:* In JCRA, the rate adjustment process is initiated periodically every  $I_{RA}$  interval by the BS which sends a rate adjustment token of  $\Delta = +\delta$  to its child nodes. For each sensor node in the network, upon reception of a rate adjustment token from its parent node, it first estimates its residual energy at the end of the current charging round:

$$\hat{e}_i = e_i - \omega (e_{tx} r_i^{out} + e_{rx} r_i^{in} + e_{sx} r_i) + \omega \hat{H}_i + \hat{A}_i, \quad (12)$$

where  $r_i$  is the data generation rate, and  $r_i^{in}$  is the measured incoming data rate. Hence, the outgoing data rate can simply be calculated as  $r_i^{out} = r_i^{in} + r_i$ . Then, depending on  $\hat{e}_i$  and the rate adjustment token received, node  $i$  behaves differently and passes tokens of different values to its child nodes. As listed in Table I, there is a total of three different cases. The rate adjustment process completes when the rate adjustment tokens reach the leaf nodes.

 TABLE I. RATE ADJUSTMENT DECISIONS AT NODE  $i$ 

Case	Condition		Action
I	$\Delta_{p,i} = \delta$	$\hat{e}_i > E_{buffer}$	$i$ may select a node from its subtree to increase the data rate by $\delta$
		$\hat{e}_i \leq E_{buffer}$	
II	$\Delta_{p,i} = -\delta$	$\hat{e}_i > E_{buffer}$	$i$ must select a node from its subtree to decrease the data rate by $\delta$
		$\hat{e}_i \leq E_{buffer}$	
		$\hat{e}_i \leq E_{buffer}$	
III	$\Delta_{p,i} = 0$	$\hat{e}_i > E_{buffer}$	$i$ may select a pair of nodes from its subtree to increase/decrease their data rates by $\delta$

*Case I:*  $\Delta_{p,i} = \delta$  and  $\hat{e}_i > E_{buffer}$ . In this case, node  $p$  has extra energy to handle more traffic while node  $i$  may be able to accommodate this request. Here,  $E_{buffer}$  represents the minimum amount of energy that each node shall possess at the end of a charging round, which is a system parameter used in JCRA to ensure that the sustainability requirement can be satisfied. Hence, node  $i$  selects a node, say  $n$ , from its neighborhood (i.e.,  $i$  and the set of its child nodes  $C_i$ ) so that (i) increment of  $n$ 's data rate results in the maximal utility gain in the neighborhood, and (ii) the sustainability requirement is maintained in the neighborhood. If  $n = i$ ,  $i$  increases its data rate to  $r_i = r_i + \delta$ . If  $n \in C_i$ ,  $i$  sets  $\Delta_{i,n} = +\delta$  and passes it to  $n$ . In addition, each node  $j \in C_i$  which is different from  $n$  is given  $\Delta_{i,j} = 0$ . Note that it is possible that neither  $i$  nor any of its child nodes has enough energy to accommodate a rate increase. In this situation,  $r_i$  remains unchanged and  $\Delta_{i,n}$

is set to 0 for each  $n \in C_i$ . Formally, we have:

$$n = \arg \max_{j \in i \cup C_i \ \& \ sc(i,j)} \{U(r_j + \delta) - U(r_j)\}, \quad (13)$$

where  $sc(i, j)$  is a Boolean value:

$$sc(i, j) = \begin{cases} \text{true} & : i = j \ \& \ \hat{e}_i - (e_{tx} + e_{sx})\delta\omega \geq E_{\text{buffer}}, \\ \text{true} & : i \neq j \ \& \ \hat{e}_i - (e_{tx} + e_{rx})\delta\omega \geq E_{\text{buffer}} \\ & \ \& \ \hat{e}_j - (e_{tx} + e_{sx})\delta\omega \geq E_{\text{buffer}}, \\ \text{false} & : \text{otherwise.} \end{cases} \quad (14)$$

*Case II:*  $\Delta_{p,i} = -\delta$  or  $\hat{e}_i \leq E_{\text{buffer}}$ . In this case, either  $p$  or  $i$  has been overloaded with too much traffic. Hence, the outgoing data rate of node  $i$  shall be reduced. To minimize utility loss due to data rate reduction, node  $i$  selects a node, say  $m$ , from its neighborhood so that the decrement of  $m$ 's data rate results in the minimal utility loss in the neighborhood. If  $m = i$ ,  $i$  reduces its data rate to  $r_i = r_i - \delta$ . If  $m \in C_i$ ,  $i$  sets  $\Delta_{i,m} = -\delta$  and passes it to  $m$ . In addition, each node  $j \in C_i$  which is different from  $m$  is given  $\Delta_{i,j} = 0$ . Formally, we have:

$$m = \arg \min_{j \in i \cup C_i} \{U(r_j) - U(r_j - \delta)\}. \quad (15)$$

*Case III:*  $\Delta_{p,i} = 0$  and  $\hat{e}_i > E_{\text{buffer}}$ . A zero-value rate adjustment token means that node  $p$  is unable to handle more traffic. In this case, node  $i$  is allowed to adjust the data generation rates within its neighborhood to increase the total utility, as long as  $i$ 's outgoing data rate remains the same. In particular, node  $i$  picks a node  $n$  according to Case I, and picks another node  $m$  according to Case II. If the utility gain is larger than the utility loss, node  $i$  updates  $r_i$ ,  $\Delta_{i,n}$ , and  $\Delta_{i,m}$  accordingly. Otherwise,  $r_i$  remains unchanged and  $\Delta_{i,j} = 0$  for each  $j \in C_i$ .

### C. Other Design Considerations

1) *JCRA Initialization:* After the data collection tree has been established, each node needs to set its initial  $r_i$  value. Considering the *diminishing return* property of the utility function, JCRA intends to set the initial data rates as evenly as possible among all sensor nodes without violating the sustainability requirement. In the following, we use an example (as shown in Figure 6) to explain how this works.

**Step 1.** As shown in Figure 6(a), each node reports its  $e_i$  and  $\hat{H}_i$  values to the BS, and derives the number of its descendant nodes ( $|D_i|$ ) by counting the number of reports it has relayed.

**Step 2.** With the collected  $e_i$  and  $\hat{H}_i$  values, the BS runs Algorithm 1 and disseminates the initial charging schedule to all nodes. In Figure 6(b), the initial charging schedule specifies that  $K = 4$  and  $\{a(s_k)\} = \{3, 1, 0, 0\}$  h.

**Step 3.** Upon reception of a charging schedule, each node estimates the total amount of energy it can receive within the current charging round as:

$$\theta_i = \hat{H}_i I_{\text{round}} + \hat{A}_i, \quad (16)$$

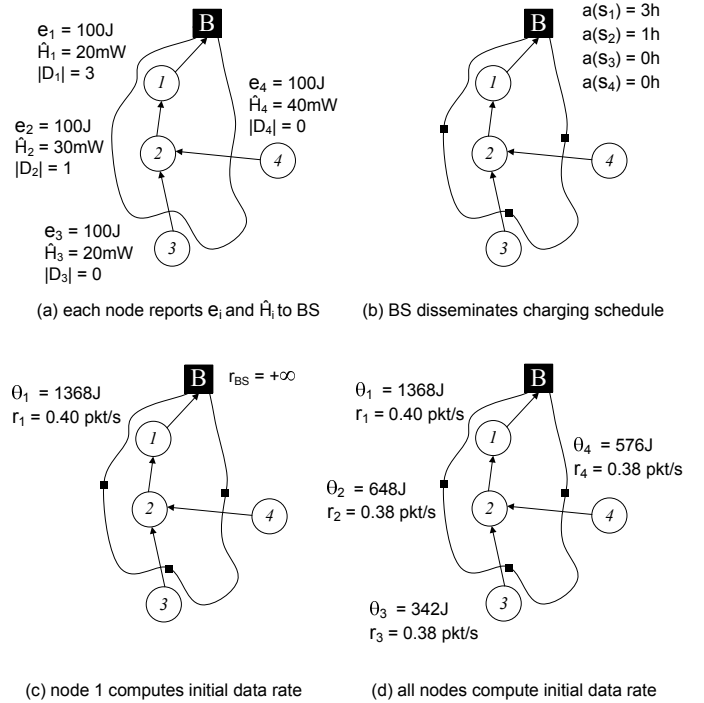


Fig. 6. An example of JCRA initialization.  $E_{\text{buffer}} = 100$  J,  $e_{tx} = 0.05$  J/pkt,  $e_{rx} = e_{sx} = 0.01$  J/pkt, and  $I_{\text{round}} = 4$  h.

where  $\hat{A}_i$  can be computed using Equation (11). During JCRA initialization, to avoid overloading a parent node, it is required that  $r_i \leq r_p$ . Hence, to satisfy the sustainability requirement:

$$\left[ \sum_{j \in D_i} (e_{tx} + e_{rx})r_j + (e_{tx} + e_{sx})r_i \right] I_{\text{round}} \leq \max\{0, e_i + \theta_i - E_{\text{buffer}}\}, \quad (17)$$

it is sufficient to set  $r_i$  as

$$r_i = \min \left\{ r_p, \max \left\{ 0, \frac{e_i + \theta_i - E_{\text{buffer}}}{[(e_{tx} + e_{rx})|D_i| + (e_{tx} + e_{sx})]I_{\text{round}}} \right\} \right\}. \quad (18)$$

This is because, with the above  $r_i$ , we have:

$$\left[ \sum_{j \in D_i} (e_{tx} + e_{rx})r_j + (e_{tx} + e_{sx})r_i \right] I_{\text{round}} \leq [(e_{tx} + e_{rx})|D_i|r_i + (e_{tx} + e_{sx})r_i]I_{\text{round}} \leq \max\{0, e_i + \theta_i - E_{\text{buffer}}\}. \quad (19)$$

In Figure 6(c), because the BS has infinite energy supply, it notifies its children nodes with  $r_{BS} = \infty$ . Node 1 computes  $\theta_1 = 1368$  J and  $r_1 = 0.40$  pkt/s, and then sends  $r_1$  to its child node 2.

**Step 4.** The above procedure continues till each node in the network has set its initial data rate, as shown in Figure 6(d).

2) *Handling of Route Dynamics:* In a real sensor network, the data collection tree may change over time. This is handled in JCRA as follows. Firstly, route changes are reflected by the measured  $r_i^{in}$  value, and the  $\hat{e}_i$  value in Equation (12) will be updated accordingly. Then, when the BS triggers a data

rate adjustment process, the rate adjustment token  $\Delta$  will be allocated according to the latest  $\hat{e}_i$  values and the network utility can be maximized with the new data collection tree. Meanwhile, each node includes its parent node information as part of the status report and sends to the BS every  $I_{MC}$  interval. This information will help the BS keep the data collection tree up to date, based on which to determine the new charging schedule for the MC.

3) *Handling of Packet Loss*: In practice, data or ACK packets may get lost due to collision, interference, or deteriorated channel condition, and a sensor node may need to retransmit multiple times before the data packet can be delivered successfully. This issue has been dealt with in JCRA by replacing  $e_{tx}$  with  $ETX_{i,p} \cdot e_{tx}$  in Equations (5), (12), and (18), where  $ETX_{i,p}$  is the expected number of transmission attempts to deliver a data packet successfully from node  $i$  to its parent node  $p$ . Note that measurement of ETX is readily available in many routing protocols such as CTP [21], and thus not an extra overhead. Similar to handling of route dynamics, each node also includes ETX as part of the status report and sends it to the BS periodically, which will be used in Equation (5) to determine the charging schedule.

4) *Overhead*: In JCRA, every  $I_{MC}$  time, each sensor node reports its current residual energy and estimated future ambient energy harvesting rate to the BS. Based on these information, the BS determines the charging schedule of the MC for the rest of the current charging round; if there is a change in the schedule, the BS notifies all sensor nodes of the updated schedule via a simple broadcast which is significantly less expensive than dissemination of node-specific rate information via unicast messages. Note that the interaction interval  $I_{MC}$  can be configured to be much larger than the sensory data report interval. As we will show in Section V, this does not compromise the network performance much as the status of the network (such as positions of the bottleneck nodes on the data collection tree) does not change very often. Therefore, the overhead incurred by JCRA may be neglected in practice.

## V. PERFORMANCE EVALUATION

### A. Simulation Setup

We have evaluated JCRA's performance in terms of *network utility* through ns-2 simulations, and compared JCRA with the centralized  $(1-\epsilon)$  approximate solution (Algorithm 1), which is denoted as CAS in this section. Note that,  $\epsilon$  is set to 10% in the comparisons. In the simulations, all sensor nodes are deployed in a 400 m  $\times$  400 m field, and the BS is located at the center. The maximal communication range of each node is 70 meters. The data collection tree connecting all the nodes is initially built by the CTP protocol [21], and RI-MAC [22] is used as the underlying MAC protocols. The node battery capacity is 10000 J and the initial nodal energy level is set to the same as system parameter  $E_{buffer}$ . Based on the default RI-MAC settings and the energy model in [23],  $e_{rx} = e_{sx} = 0.02$  J/pkt and  $e_{tx}$  is 0.05 J/pkt.

The predefined moving trajectory is a closed curve with the BS as the start and end point. The energy charging efficiency

model follows Equation (2) with the charging output power  $\Lambda_c$  of 3 W. The MC moving speed  $v_{MC}$  is 1 m/s. Among the sensor nodes, a certain percent of them are randomly deployed within a chargeable distance (i.e.,  $D_{max}$  in Equation (2)) from the trajectory and these nodes are called near-trajectory nodes. Each node also harvests energy from the ambient energy source according to a node-specific profile. The utility function  $U(r)$  is set as  $1 - e^{-r}$ . In JCRA, the BS triggers an adaptation round every five minutes, for which system parameter  $\delta$  is set to 0.05 pkt/s.

### B. Simulation Results

In this section, the results plotted in each figure are averaged over the simulations conducted with 30 randomly generated topologies, and each simulation lasts for 72 hours.

1) *Network utility with varying energy buffer*: Figure 7 compares the performance of JCRA and CAS when energy buffer ( $E_{buffer}$ ) varies from 1000 J to 9000 J. According to Figure 7(a), JCRA performs the best when  $E_{buffer}$  is 3000 J, while the performance becomes lower when  $E_{buffer}$  is larger or smaller. The phenomenon is explained as follows.

As discussed in Section III,  $E_{buffer}$  defines an energy buffer to tolerate environmental and network uncertainties. When it is too small (e.g.,  $E_{buffer} = 1000$  J), some nodes may run out of energy due to, for example, inaccurate estimation of solar harvesting or wireless charging rate. If a node depletes its energy, all data packets generated in its subtree cannot be forwarded to BS before the node regains energy, and so the network utility is degraded. On the other hand, when  $E_{buffer}$  is too large (e.g.,  $E_{buffer} = 9000$  J), a node may hold much residual energy when a charging round starts. In this case, its energy repository could hit the battery ceiling (10000 J in the simulation) if there is a high solar harvesting or wireless charging rate. Hence, the available energy supply may not be fully utilized. Only when  $E_{buffer}$  is set to a proper value, the problem of energy depletion or in-efficient utilization can be alleviated, and thus a high network utility can be achieved. Particularly in this simulation, when  $E_{buffer} = 3000$  J and  $E_{buffer} = 5000$  J, JCRA achieves 86% and 85% of the network utility archived by CAS, respectively.

In addition, Figure 7(b) plots the temporally-varying traces of the minimal nodal energy during one simulation run, which shows that the network sustainability requirement is satisfied; that is, the residual energy of every node is no less than  $E_{buffer}$  at the end of a charging round.

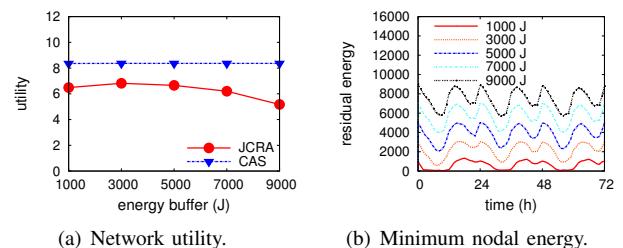


Fig. 7. Performance comparison as  $E_{buffer}$  varies. Setting:  $I_{round} = 12$  h,  $I_{MC} = 3$  h, 60 nodes are in the network including 30 near-trajectory nodes.

2) *Network utility with varying charging round length*: As we can see from Figure 8, the sustainability can be satisfied as charging round length ( $I_{\text{round}}$ ) varies (shown in Figure 8(b)), but the network utilities achieved by both JCRA and CAS decrease when  $I_{\text{round}}$  increases (shown in Figure 10(a)). This phenomenon can be explained as follows.

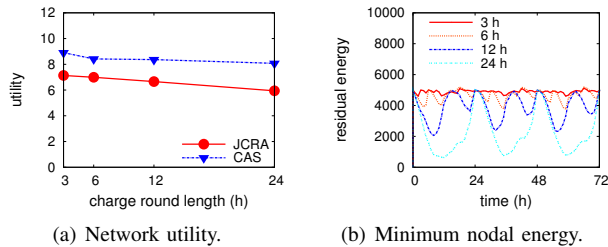


Fig. 8. Performance comparison as  $I_{\text{round}}$  varies. Setting:  $E_{\text{buffer}} = 5000$  J,  $I_{MC} = 3$  h, 60 nodes are in the network including 30 near-trajectory nodes.

To satisfy the sustainability requirement, each node  $i$  should keep estimating its nodal energy level at the end of the current charging round, denoted as  $\hat{e}_i$ , and ensure  $\hat{e}_i \geq E_{\text{buffer}}$ . Due to dynamic changes in solar energy harvesting rate and other network conditions,  $\hat{e}_i$  estimated by node  $i$  may deviate from the actual value, and the estimation error has negative impact on the network utility. Specifically, if  $\hat{e}_i$  is smaller than the actual value, the node will be reluctant to spend its energy to achieve higher network utility; moreover, the reluctance in energy spending may also increase the probability for its battery to hit the energy ceiling, resulting in energy waste and thus lower the network utility. On the other hand, if  $\hat{e}_i$  is higher than the actual value, the node will spend energy too fast, which may result in energy depletion, which can also decrease the network utility.

As the estimation error can accumulate over time, the longer is the charging round, the larger is the estimation error, and hence the less efficiency in performance.

3) *Network utility with varying charging rescheduling interval*: Since the charging activity in CAS is not rescheduled during a charging round, the network utility achieved by CAS does not change when the charging rescheduling interval ( $I_{MC}$ ) varies. On the other hand, as shown in Table II, JCRA yields a higher network utility with charging rescheduling (e.g.,  $I_{MC} = 1, 3, 6$  h) than without rescheduling (i.e.,  $I_{MC} = 12$  h is the same as the charging round). This is because rescheduling can remedy the difference between the estimated ambient energy harvesting rate and the actual one. However, the rescheduling frequency does not have a big impact on the performance improvement. This is due to the fact that, the MC is mainly scheduled to charge communication bottleneck nodes, of which only a small portion of energy consumption can be compensated solely through ambient energy harvesting. The set of communication bottleneck nodes on the data collection tree is fairly stable. Hence, the rescheduling process does not make significant changes to the charging schedule. To summarize, we can see that it is beneficial to perform charging rescheduling, but the interval  $I_{MC}$  needs not to be very small.

4) *Network utility with varying network density*: The impact of network density on JCRA's performance is shown in

TABLE II. ACHIEVED NETWORK UTILITY AS  $I_{MC}$  VARIES.

$I_{MC}$	JCRA	CAS
1h	6.82	8.36
3h	6.89	8.36
6h	6.86	8.36
12h (w/o rescheduling)	6.73	8.36

Figure 9. As more and more sensor nodes are deployed to generate data, the network utility achieved by both CAS and JCRA increases. Also, JCRA can achieve around 80% of the network utility achieved by CAS.

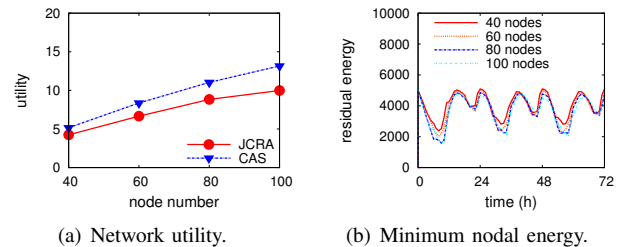


Fig. 9. Performance comparison as the network size varies. Setting:  $E_{\text{buffer}} = 5000$  J,  $I_{\text{round}} = 12$  h,  $I_{MC} = 3$  h, and 50% of the nodes are near-trajectory.

5) *Network utility with varying percentage of near-trajectory nodes*: Figure 10 compares the performance of JCRA and CAS when the percentage of the near-trajectory nodes varies from 25% to 100%. As more nodes are deployed near the trajectory, the MC has larger impact over the energy distribution and hence the data rate generation of the network. Therefore, the achieved network utility by both JCRA and CAS increases. It can also be observed that, the network utility achieved by JCRA is around 80% of CAS regardless of the percentage of near-trajectory nodes among all nodes.

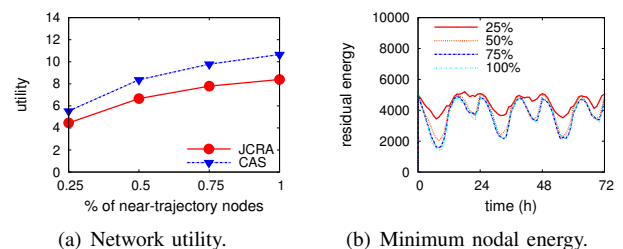


Fig. 10. Performance comparison as the percentage of near-trajectory nodes varies. Setting:  $E_{\text{buffer}} = 5000$  J,  $I_{\text{round}} = 12$  h,  $I_{MC} = 3$  h, and 60 nodes are in the network.

## VI. RELATED WORKS

*Data rate adaption schemes for sensor networks harvesting ambient energy*. To deal with the time-varying nature of ambient energy source such as solar, schemes have been proposed to adapt sensory data rates according to ambient energy availability. Particularly, Fan et al. [7] proposed to maximize the lexicographic rate assignment to sensor nodes. Moser et al. [8] proposed a rate control approach for a single energy harvesting node to maximize the average sensing rate over time. Noh and Kang [9] proposed a flow control algorithm to maximize the amount of data collected over the network.

However, these works all assume the system utility increases linearly as the data rate. To be more applicable in practical scenarios, the system utility has been modeled as a concave and non-decreasing function of data rate [10], [11]. Under such a model, Liu et al. [10] proposed a dual decomposition and subgradient method based algorithm, called QuickFix, to compute data sampling rates, and Zhang et al. [11] proposed an optimal centralized rate allocation algorithm and a distributed protocol to maximize total utility achieved by all nodes, while ensuring eternal network lifetime. Different from JCRA, all these works only passively adapt sensory data rate to changes in ambient energy availability, and hence do not achieve the optimal or near-optimal network utility as JCRA does.

*Charging scheduling and data rate adaption schemes for wireless chargeable sensor networks.* As wireless charging technology advances, it has been technically feasible for a mobile robot to carry a wireless charger (MC) and deliver energy to where it is needed [4], [12]. Peng et al. [13] built a prototype system to study the feasibility of using the wireless charging technology for prolonging sensor network lifetime. Shi et al. [14] conducted a theoretical study and proposed a static, centralized joint routing and charging scheme to maximize the MC's vacation time. To handle practical issues such as limited charging capability, and heterogeneous node attributes, a joint routing and charging scheme named J-RoC is proposed in [5] to maximize the network lifetime. Compared to the charging model used in JCRA, the above works all assume that the MC can only charge one node at a time, which does not fully utilize the broadcast nature of the wireless energy transfer. Based on the simultaneous charging model, Tong et al. [15] proposed to jointly determine the sensor node deployment and routing strategies to minimize the overall energy consumption at the chargers. Xie et al. [16] proposed to jointly optimize the traveling path, routing flow and charging time. However, all the aforementioned works assume that the MC can move to anywhere in the deployment field without constraint, and such assumption may not hold in practice. Xie et al. [6] also studied the problem of co-locating the mobile base station and the MC, where the MC can only move along some pre-plan trajectory; but the goal was to minimize the overall energy consumption while maintaining system sustainability, which is different from JCRA's goal of maximizing the network utility. Note that, ambient energy harvesting has not been considered in the works falling into this category.

Compared to the above works, JCRA is unique in: it considers together three factors, uncontrollable ambient energy harvesting, controllable wireless charging, and controllable sensory data adaption, to optimize network utility while keeping the network sustainable. To our knowledge, this is the first effort that systematically studies all these factors.

## VII. CONCLUSION

This paper presents JCRA to maximize the network utility while ensuring eternal network lifetime. We present the design and implementation of the JCRA scheme and show its effectiveness in improving the network utility compared with a centralized,  $(1 - \epsilon)$  optimal solution via ns-2 simulations, under various configurations.

## ACKNOWLEDGEMENT

This work is supported partly by the NSF under grants CNS-0831874 and EECs-1128312, and by the ONR under grant N00014-09-1-0748.

## REFERENCES

- [1] A. Kansal, D. Potter, and M. Srivastava, "Performance Aware Tasking for Environmentally Powered Sensor Networks," *SIGMETRICS Perform. Eval. Rev.*, vol. 32, no. 1, pp. 223–234, 2004.
- [2] C. Park and P. Chou, "AmbiMax: Autonomous Energy Harvesting Platform for Multi-Supply Wireless Sensor Nodes," in *SECON*, 2006.
- [3] S. Jose, J. Mur-mir, R. Amirtharajah, A. Ch, and J. Lang, "Vibration-to-electric energy conversion," *IEEE Transactions on VLSI Systems*, vol. 9, no. 1, pp. 64–76, 2001.
- [4] Powercast, "Online link," <http://www.powercastco.com>.
- [5] Z. Li, Y. Peng, W. Zhang, and D. Qiao, "J-RoC: a Joint Routing and Charging Scheme to Prolong Sensor Network Lifetime," in *ICNP*, 2011.
- [6] L. Xie, Y. Shi, Y. Hou, W. Lou, H. Sherali, and S. Midkiff, "Bundling Mobile Base Station and Wireless Energy Transfer: Modeling and Optimization," in *INFOCOM*, 2013.
- [7] K. Fan, Z. Zheng, and P. Sinha, "Steady and Fair Rate Allocation for Rechargeable Sensors in Perpetual Sensor Networks," in *SenSys*, 2008.
- [8] C. Moser, L. Thiele, D. Brunelli, and L. Benini, "Adaptive Power Management for Environmentally Powered Systems," *Computers, IEEE Transactions on*, vol. 59, no. 4, pp. 478–491, 2010.
- [9] D. Noh and K. Kang, "A Practical Flow Control Scheme Considering Optimal Energy Allocation in Solar-Powered WSNs," in *ICCCN*, 2009.
- [10] R. Liu, P. Sinha, and C. Koksall, "Joint Energy Management and Resource Allocation in Rechargeable Sensor Networks," in *INFOCOM*, 2010.
- [11] B. Zhang, R. Simon, and H. Aydin, "Maximum utility rate allocation for energy harvesting wireless sensor networks," in *MSWiM*, 2011.
- [12] A. Kurs, A. Karalis, M. Robert, J. Joannopoulos, P. Fisher, and M. Soljacic, "Wireless Power Transfer via Strongly Coupled Magnetic Resonances," *Science*, vol. 317, pp. 83–86, 2007.
- [13] Y. Peng, Z. Li, W. Zhang, and D. Qiao, "Prolonging Sensor Network Lifetime Through Wireless Charging," in *RTSS*, 2010.
- [14] Y. Shi, L. Xie, Y. Hou, and H. Sherali, "On Renewable Sensor Networks with Wireless Energy Transfer," in *INFOCOM*, 2011.
- [15] B. Tong, Z. Li, G. Wang, and W. Zhang, "How Wireless Power Charging Technology Affects Sensor Network Deployment and Routing," in *ICDCS*, 2010.
- [16] L. Xie, Y. Shi, Y. Hou, W. Lou, H. Sherali, and S. Midkiff, "On Renewable Sensor Networks with Wireless Energy Transfer: The Multi-Node Case," in *SECON*, 2012.
- [17] X. Wang and K. Kar, "Cross-layer rate control for end-to-end proportional fairness in wireless networks with random access," in *MobiHoc*, 2005.
- [18] L. Su, Y. Gao, Y. Yang, and G. Cao, "Towards optimal rate allocation for data aggregation in wireless sensor networks," in *MobiHoc*, 2011.
- [19] Ipopt, "Online link," <https://projects.coin-or.org/Ipopt>.
- [20] A. Cammarano, C. Petrioli, and D. Spenza, "Pro-Energy: A novel energy prediction model for solar and wind energy-harvesting wireless sensor networks," in *MASS*, 2012.
- [21] O. Gnawali, R. Fonseca, K. Jamieson, D. Moss, and P. Levis, "Collection Tree Protocol," in *SenSys*, 2009.
- [22] Y. Sun, O. Gurewitz and D. Johnson, "RI-MAC: a receiver-initiated asynchronous duty cycle MAC protocol for dynamic traffic loads in wireless sensor networks," in *SenSys*, 2008.
- [23] Z. Li, Y. Peng, D. Qiao, and W. Zhang, "Joint Aggregation and MAC Design to Prolong Sensor Network Lifetime," in *ICNP*, 2013.